Electronic Supplementary Material (ESI) for Journal of Materials Chemistry A.

Supporting Information:

Time evolution studies of dithieno[3,2-b:2',3'-d]pyrrole-based A-D-A oligothiophene bulk heterojunctions during solvent vapor annealing towards optimization of photocurrent generation

Sadok Ben Dkhil,[a] Martin Pfannmöller,[b] Ibrahim Ata,[c] David Duché,[d] Meriem Gaceur,[a] Tomoyuki Koganezawa,[e] Noriyuki Yoshimoto,[f] Jean-Jacques Simon,[d] Ludovic Escoubas,[d] Christine Videlot-Ackermann,[a] Olivier Margeat,[a] Sara Bals,*[,b] Peter Bäuerle,*[,c] and Jörg Ackermann*[,a]

[a] Aix Marseille Université, CNRS UMR 7325, CINaM, Marseille, France

[b] Electron Microscopy for Materials Research (EMAT), University of Antwerp, Groenenborgerlaan 171, 2020 Antwerp, Belgium

[c] University of Ulm, Institute of Organic Chemistry II and Advanced Materials Albert-Einstein-Allee 11, 89081 Ulm, Germany

[d] Aix Marseille Univ, Univ Toulon, CNRS, IM2NP, Marseille, France

[e] Industrial Application Division, Japan Synchrotron Radiation Research, Institute (JASRI), Sayo, Hyogo 679-5198, Japan

[f] Department of Materials Science and Engineering, Iwate University, Ueda Morioka 020 8551, Japan.

Content:

A: Experimental section
B: Figures S1-S8
C: Tables S1-S4

A: Experimental Section

Materials:

1 molecule was synthesized following procedure published previously.[1] ZnO nanocrystals. ZnO nanocrystals were prepared as published elsewhere.[2] The solution-processable n-type semiconductor inks were prepared by transferring the as-synthesized ZnO nanoparticles from methanol to isopropanol (IPA) mixed with ethanolamine (0.2 vol.%) (EA).[2] By this technique, cluster free ZnO nanocrystal solutions in isopropanol of concentration of 2-20 mg/mL were prepared. $PC_{71}BM$ of 99% purity was purchased from Nano-C.

Solar Cell Fabrication and Characterization:

Solar cells in normal device structure were processed as follow. First, ITO substrates (purchased from LUMTEC) were thoroughly cleaned by sonication in acetone and ethanol followed by rinsing with water, then sonication in isopropanol and applying ultraviolet-ozone for 10 min. A thin layer of poly(3,4- PEDOT:PSS) (CLEVIOS AI 4083) was spin-coated on the cleaned ITO pre-coated glass substrate at the speed of 4000 rpm for 60 s followed by heating on a hot-plate at 140°C for 15 min. The substrates were then transferred to nitrogen filled glove box. The **1**:$PC_{71}BM$ active blend layer was prepared by spin-coating a chloroform solution containing **1** and $PC_{71}BM$ at different mass ratios (concentration of **1** was kept constant at 5 $mg.mL^{-1}$) at 1500 rpm for 2 min. Solvent vapor annealing (SVA) was used to modify the blend morphology by exposing the cell to chloroform atmosphere in a petri dish with controlled duration (SVA time). After this process, the ZnO nanoparticles in isopropanol containing 0.2% (v/v) ethanolamine were spincoated on the top of active layers at 1500 rpm for 1 min and dried on a hot plate at 80°C for 2 min. Depending on the ZnO concentration, it was possible to adjust the thickness from 10 to 70 nm. For processing the cathode, Al metal electrodes (100 nm) were thermally evaporated at 1×10^{-7} mbar through a shadow mask and the device area was 0.27 cm^2. The current density–voltage (J–V) characteristics of the devices were measured using a Keithley 238 Source Measure Unit inside the glovebox using Lumtec substrates. Solar cell performance was measured by using a Newport class AAA 1.5 Global solar simulator (Oriel Sol3ATMmodel n_ 94043A) with an irradiation intensity of 100 $mW.cm^{-2}$. The light intensity was determined with a Si reference cell (Newport Company, Oriel n_94043A) calibrated by National Renewable Energy Laboratory (NREL). Shadow masks were used to well-define the illuminated area to 0.27×1.0 cm^2. Comparison of masked and unmasked solar cells gave consistent results with photocurrent increase by less 2% for unmasked devices. Performance of the best devices were presented, while average PCEs were obtained with standard deviation analysis calculated using 9 devices and are shown in the Tables S1, S2 and S3. External quantum efficiency (EQE) measurements were performed in air using a homemade setup consisting of a Keithley 238 Source Measure Unit and Newport monochromator. Light intensity was measured with a calibrated Si-diode from Newport Company.

Morphological analysis:

The surface morphology of the **1**:$PC_{71}BM$ blend layers was studied by atomic force microscopy (AFM) using a Nanoscope III in taping mode before and after SVA of different process times.

Pure **1** layers and **1**:$PC_{71}BM$ blend layers were further analysed by 2D-GIXD with high-brightness synchrotron radiation at BL19B2 in SPring-8. 2D-GIXD measurements were performed using a high-sensitive 2D X-ray detector (PILATUS 300K) equipped with a Soller slit. The incident angle and wavelength of X-rays were 0.13° and 0.100 nm, respectively.

STEM-SI analyses were performed using HyperSpy (http://hyperspy.org), which is an open-source library for treatment of multi-dimensional data sets. STEM measurements were performed with a Titan 60-300 microscope (FEI) at 120 kV, equipped with an Enfinium spectrometer (Gatan). Data sets of blends in lateral dimensions were recorded on samples of photoactive layers prepared on PEDOT:PSS. Floated on top of deionized water dissolved the PEDOT:PSS so that pieces of the **1**:fullerene blends were captures by a standard microscopy grid covered with a holey carbon film (QUANTIFOIL®). Cross-sections were prepared from complete devices using a Helios Nanolab 650 (FEI). For STEM-SI imaging a scanning step size of 3 nm was chosen, 1.5 nm for the cross-sectional analyses.

Optical simulations of SM solar cells:

First, spectroscopic ellipsometric (SE) measurements were performed on all layers of the solar cell using a rotating-polarizer ellipsometer (Semilab GES5).[3,4] In this specific work, SE measurement were performed on **1**:PC$_{71}$BM layers coated on Si substrates with a 333 nm thick SiO$_2$ layer as the refractive index differences between the silicon substrate, the SiO$_2$ layer, and the organic films is high enough to ensure high reflection coefficients at the Si/SiO$_2$/organic interfaces.[3,4] SEA software (Semilab company) was used to fit the SE measurements of tan(Ψ) and cos(Δ) and extract the optical indices n(λ) and k(λ) of the materials.[2] The dielectric functions ($\varepsilon = \varepsilon_1 + i * \varepsilon_2 = (n + i*k)^2$) of **1**:PC$_{71}$BM have been fitted with a sum of Gaussian oscillators which is suitable to describe strong electron-phonon coupling in π-conjugated molecules.[5]

This technique is indirect since it needs data analysis. The data analysis requires an optical model corresponding to the structure of the sample. Each layer is defined by dielectric functions (or optical indices) and thickness. To evaluate our dispersion model, two criteria were used. The first criteria was the root mean square error given by the SEA software (From SemiLab) between measured and calculated data which must be minimized (see Table S4 and Figure S5*). The second criteria was the fit to the transmission, reflection and absorption spectra of films coated on glass (see the paragraph dedicated to *Optical Measurements*). Layer thicknesses were determined with a mechanical profilometer in combination with AFM cross-section measurements (see Table S4). Optical simulations of the light distribution inside the solar cell have been performed using a transfer matrix method (TMM). The input parameters of our optical model are the optical indices n and k of the materials obtained by SE and the thicknesses of the films. For the TMM calculations, we considered a device architecture consisting in a stack composed by a 150 nm thick indium tin oxide (ITO) layer, a 40 nm PEDOT:PSS interface layer, a **1**:$PC_{71}BM$ layer, a ZnO layer of varying thickness and a 100 nm back electrode in Aluminum (see Figure S5).

Optical Measurements:

The optical measurements of the refllexion, the transmission and the absorption spectra were obtained by using a lambda 950 UV/Vis spectrophotometer from Perkin Elmer equipped with an integrating sphere (see Figure S5**). The total reflection (transmission) spectrum $R(\lambda)$ ($T(\lambda)$) is defined as the ratio of the light intensity reflected by the sample $I_r(\lambda)$ (transmitted through the sample $I_t(\lambda)$) to the total incident intensity $I_0(\lambda)$ ($R(\lambda)=100*I_r(\lambda)/I_0(\lambda)$ and $T(\lambda)=100*I_t(\lambda)/I_0(\lambda)$). The absorption spectrum $A(\lambda)$ can be then calculated using the following formula: $A(\lambda) = 100 - R(\lambda) - T(\lambda)$.

B: Figures

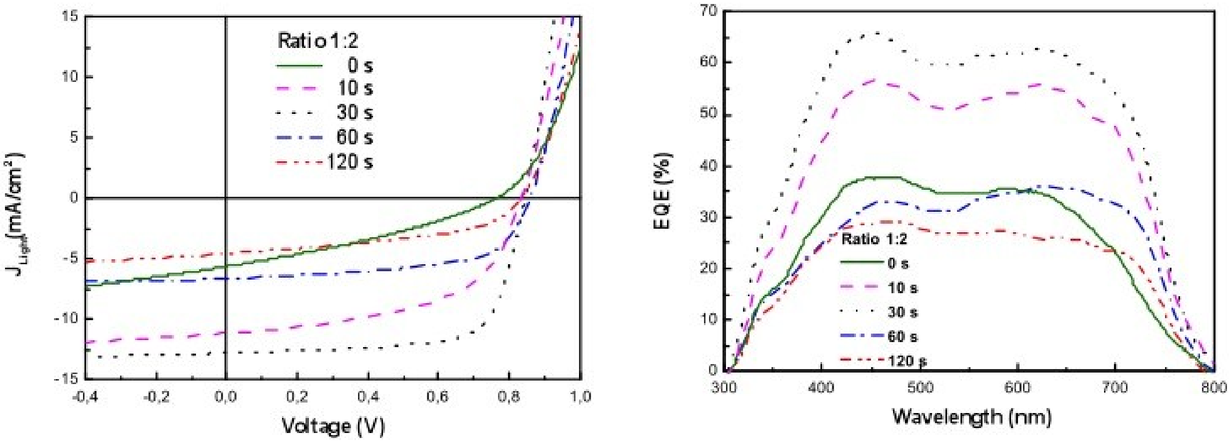

Figure S1. J-V curves (left) and EQE measurements (right) for solar cells using the ratio 1:2 for **1**:$PC_{71}BM$ blend as a function of SVA time.

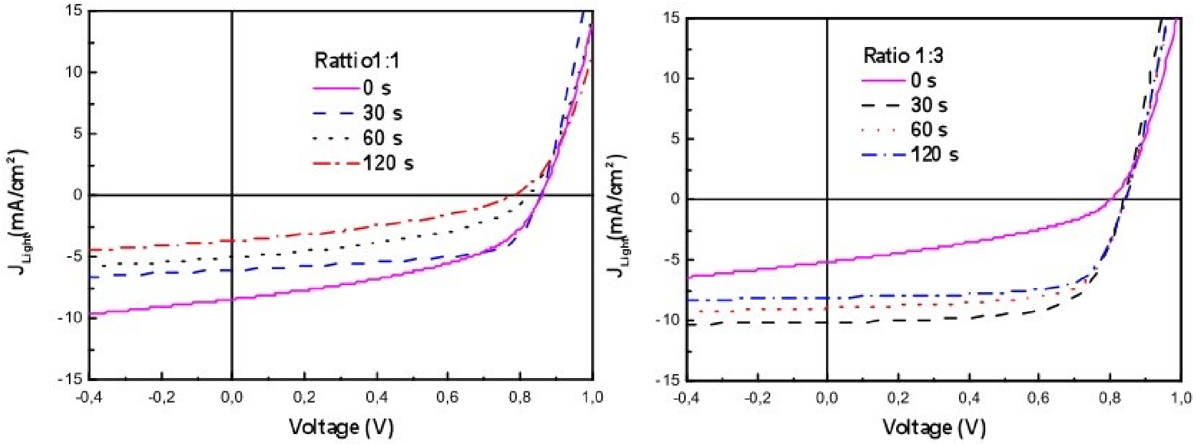

Figure S2. J-V curves for solar cells using different **1**:$PC_{71}BM$ ratios as a function of SVA time: 1:1 (left) and 1:3 (right).

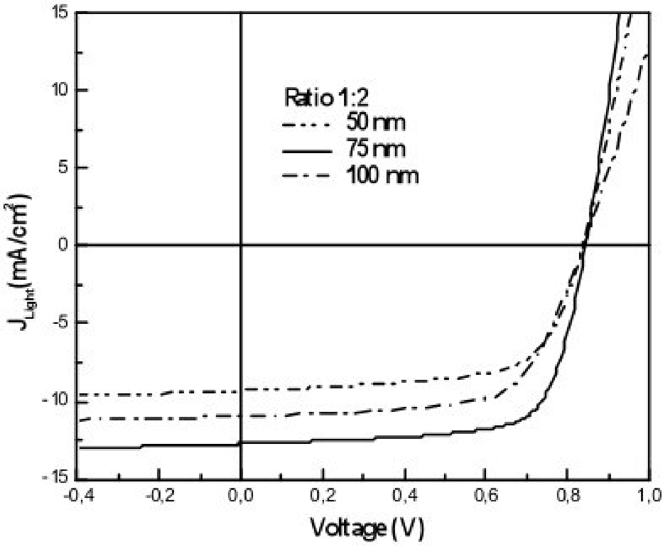

Figure S3. J-V curves for solar cells using 1:2 as **1**:$PC_{71}BM$ ratio and 30 s SVA time as a function of blend layer thickness.

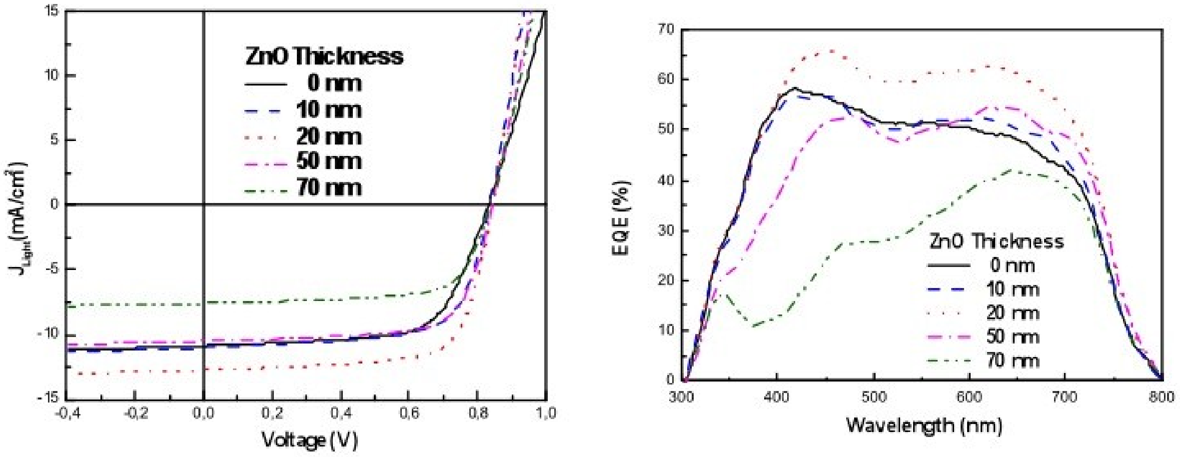

Figure S4. J-V curves (left) and EQE measurements (right) for solar cells using 1:2 as **1**:PC$_{71}$BM ratio and 30 s SVA time as a function of ZnO optical layer thickness.

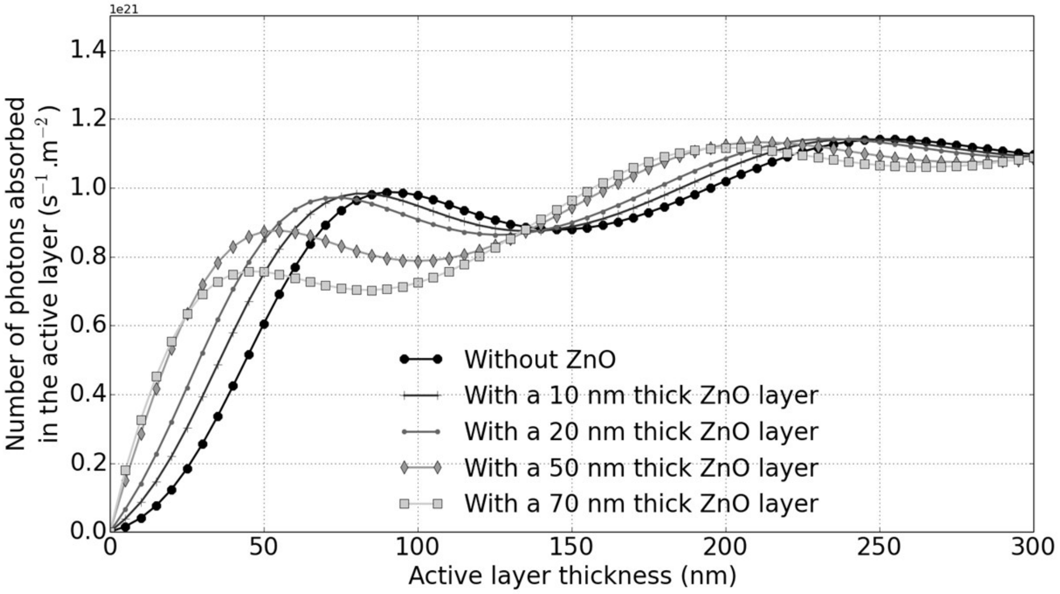

Figure S5. Theoretical absorption in the active layer as a function of active layer thickness for different ZnO optical layer thicknesses.

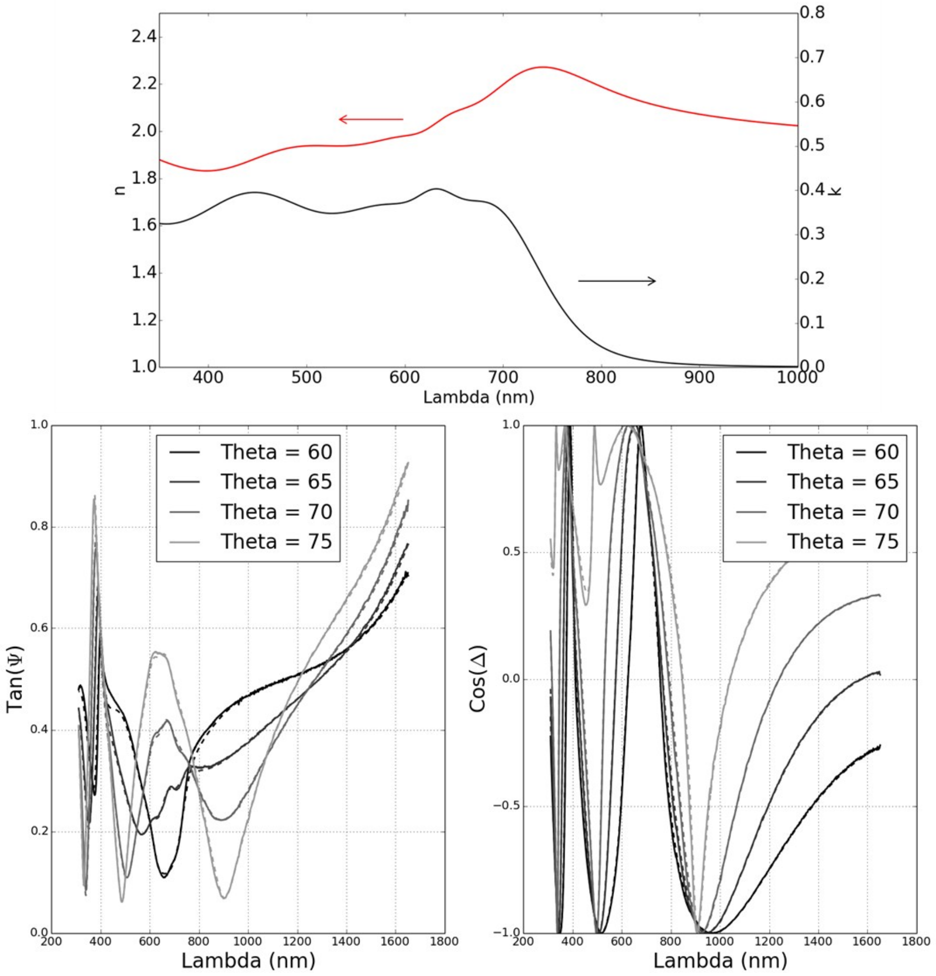

Figure S5*. (Top) optical constants n and k of **1**:$PC_{71}BM$ obtained by spectroscopic ellipsometry. (Down) Measured and calculated ellipsometric angles tan(Ψ) and cos(Δ) at four incident angles (Theta) for a 63 nm thick **1**:$PC_{71}BM$ film coated on silicon substrates with a 333 nm thick SiO_2 layer. The results show excellent agreement between the measurements and the calculation.

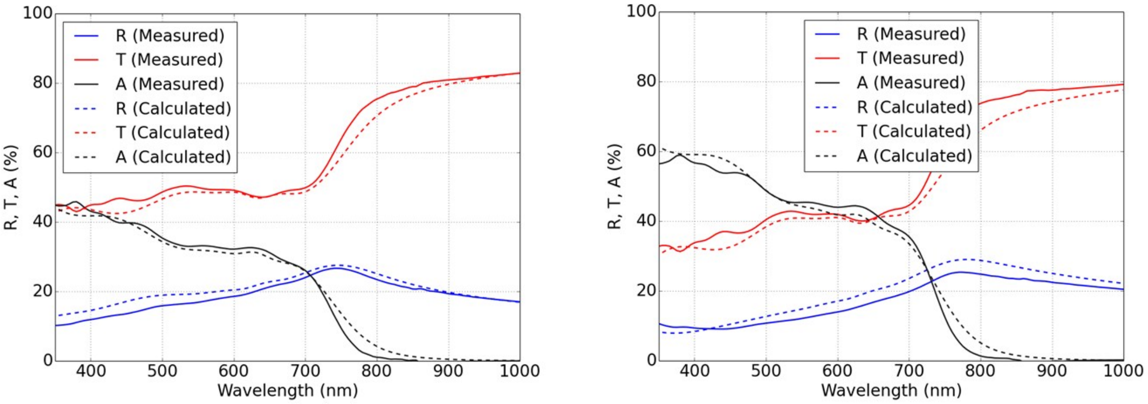

Figure S5**. Calculated and experimental absorption, transmission and reflection spectra of a 62 nm thick (left) and 92 nm thick **1**:PC$_{71}$BM film coated on glass.

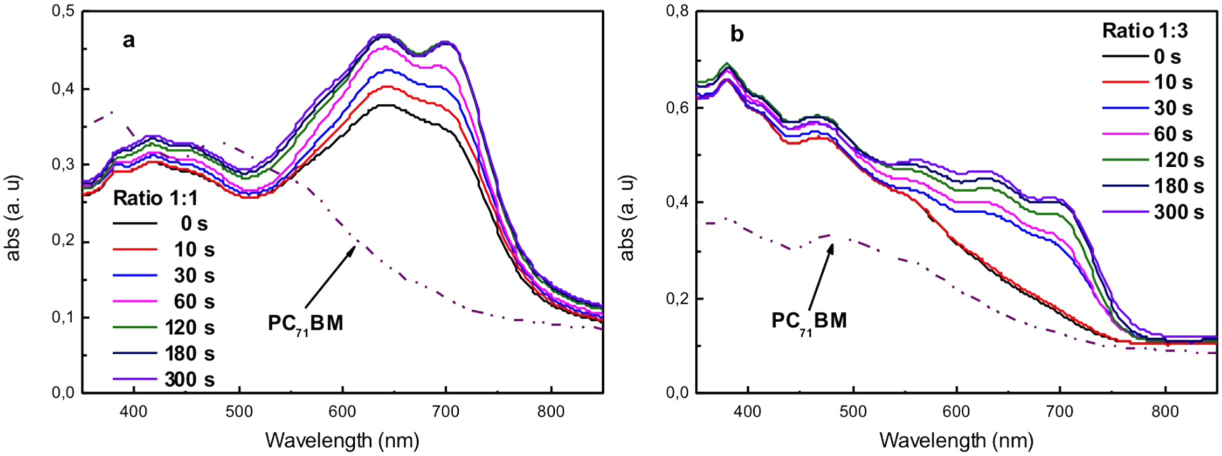

Figure S6. Absorption spectra of **1**:PC$_{71}$BM blends with a mass ratio of 1:1 (a) and 1:3 (b) as a function of SVA time.

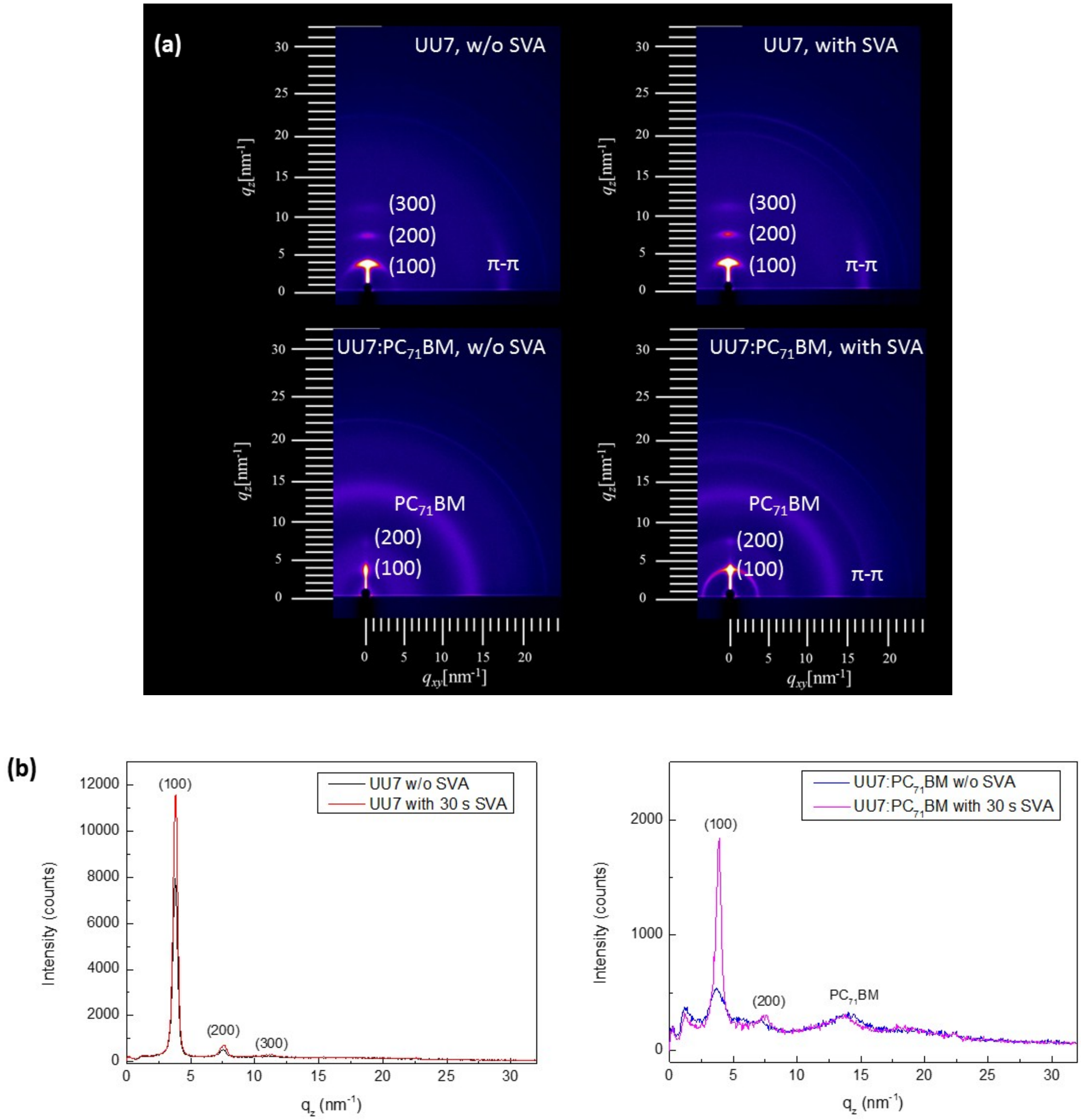

Figure S7. (a) Two dimensional diffraction patterns of pure **1** layers and **1**:PC$_{71}$BM blend layers before and after a 30 s SVA treatment. (b) Profiles along the (100) peak before and after the 30 s SVA treatment of pure **1** layers and **1**:PC$_{71}$BM blend layers.

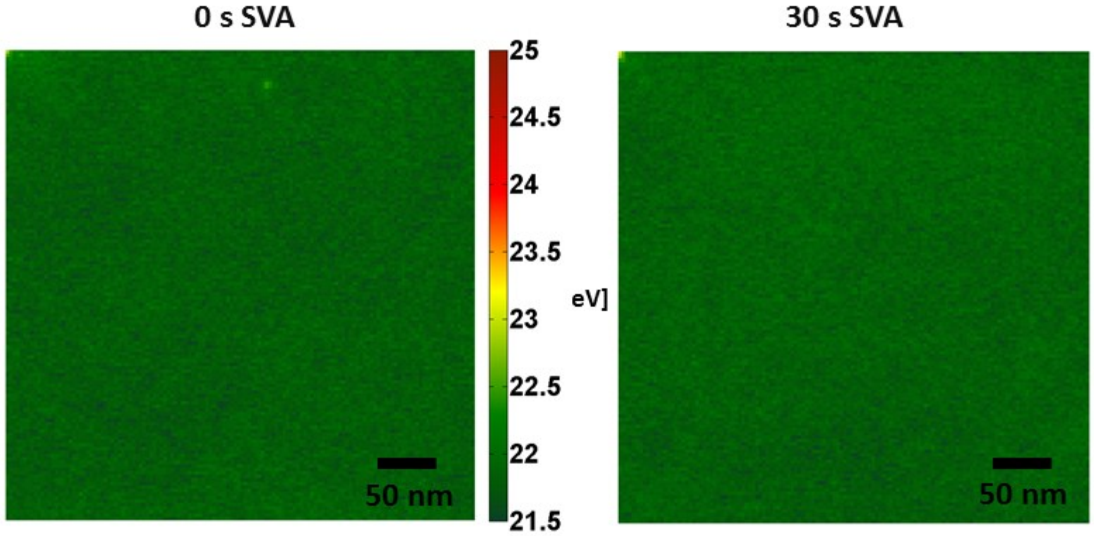

Figure S8. Plasmon peak maps for 1 films as-casted (0 s SVA) and after 30 s SVA. The mean plasmon peak position for both is approximately 21.8 eV.

C: Tables

Table S1. Photovoltaic parameters of solar cells using different **1**:$PC_{71}BM$ ratios as a function of SVA time: 1:1 and 1:3.

Ratio 1:1					
SVA duration	**PCE (%)**	**V_{oc} (mV)**	**J_{sc} (mA.cm^{-2})**	**FF (%)**	**Average PCE (± std. dev.)**
0 s	3.30	858	8.37	46	3.15±0.12
30 s	3.18	857	6.03	62	3.01±0.16
60 s	1.74	822	4.96	43	1.50±0.21
120 s	0.99	778	3.62	35	0.61±0.31
Ratio 1:3					
SVA duration	**PCE (%)**	**V_{oc} (mV)**	**J_{sc} (mA.cm^{-2})**	**FF (%)**	**Average PCE (± std. dev.)**
0 s	1.50	801	5.10	37	1.35±0.13
30 s	5.66	838	10.1	67	5.40±0.22
60 s	5.07	843	8.89	68	4.89±0.16
120 s	4.75	843	8.04	70	4.35±0.28

Table S2. Photovoltaic parameters of solar cells using 1:2 as **1**:$PC_{71}BM$ ratio as a function of ZnO thickness.

ZnO Thickness (nm)	**PCE (%)**	**V_{oc} (mV)**	**J_{sc} (mA.cm^{-2})**	**FF (%)**	**Average PCE (± std. dev.)**
0	5.99	831	10.8	66	5.84±0.16
10	6.32	836	11.0	69	6.08±0.18
20	7.74	844	12.7	72	7.57±0.13
50	6.30	845	10.5	71	6.02±0.26
70	4.44	837	7.5	70	3.98±0.29

Table S3. Photovoltaic parameters of solar cells using 1:2 as **1**:PC$_{71}$BM ratio and 30 s SVA time as a function of active layer thickness.

Active layer Thickness (nm)	PCE (%)	V_{oc} (mV)	J_{sc} (mA.cm^{-2})	FF (%)	Average PCE (± std. dev.)
100	6.01	839	10.9	65	5.88±0.16
75	7.74	844	12.7	72	7.57±0.13
50	5.15	836	9.3	66	4.88±0.24

Table S4. Parameters for the model of the imaginary part of the dielectric function for the 63 nm PC$_{71}$BM film.

Peaks	Energy (eV)	Amplitude (a.u.)	Broadening (eV)
Gaussian 1	2.580	1.050	0.914
Gaussian 2	2.012	0.949	0.497
Gaussian 3	1.951	0.259	0.136
Gaussian 4	3.248	0.616	1.268
Gaussian 5	5.629	3.666	2.633
Gaussian 6	1.765	0.899	0.229
$\varepsilon(\infty)$		1.771	
Thickness (nm)		63	
Thickness profilo. (nm)		66	
RMSE		0.01745	

<u>References</u>:

1. C. D. Wessendorf, G. L. Schulz, A. Mishra, P. Kar, I. Ata, M. Weidelener, M. Urdanpilleta, J. Hanisch, E. Mena-Osteritz, M. Lindén, E. Ahlswede, and P. Bäuerle, *Adv. Energy Mater.*, 2014, **4**, 1400266.

2. S. Ben Dkhil, D. Duche, M. Gaceur, S. Ben Dkhil, D. Duché, M. Gaceur, A. K. Thakur, F. B. Aboura, L. Escoubas, J.-J. Simon, A. Guerrero, J. Bisquert, G. Garcia-Belmonte, Q. Bao, M. Fahlman, C. Videlot-Ackermann, O. Margeat, and J. Ackermann, *Adv. Energy Mater.*, 2014, **4**, 1400805.

3. D. Duché, F. Bencheikh, S. Ben Dkhil, M. Gaceur, N. Berton, O. Margeat, J. Ackermann, J. J. Simon, and L. Escoubas, *Sol. Energy Mater. Sol. Cells*, 2014, **126**, 197–204.

4. L. A. A. Pettersson, L. S. Roman, O. Inganäs, and O. Inganäs, *J. Appl. Phys.*, 1999, **86**, 487.

5. F. Bencheikh Aboura, D. Duché, J. J. Simon, and L. Escoubas, *Chem. Phys.*, 2015, **450-451**, 102–108.